To appear in Astrophysical Journal Letters

Extreme host galaxy growth in powerful early-epoch radio galaxies

Peter Barthel

Kapteyn Astronomical Institute, University of Groningen, The Netherlands

pdb@astro.rug.nl

Martin Haas

Astronomisches Institut, Ruhr Universität, Bochum, Germany

Christian Leipski

Max-Planck-Institut für Astronomie, Heidelberg, Germany

and

Belinda Wilkes

Harvard-Smithsonian Center for Astrophysics, Cambridge, Massachusetts, USA

ABSTRACT

During the first half of the universe's age, a heyday of star-formation must have occurred because many massive galaxies are in place after that epoch in cosmic history. Our observations with the revolutionary Herschel Space Observatory[1] reveal vigorous optically obscured star-formation in the ultra-massive hosts of many powerful high-redshift 3C quasars and radio galaxies. This symbiotic occurrence of star-formation and black hole driven activity is in marked contrast to recent results dealing with Herschel observations of X-ray selected active galaxies. Three archetypal radio galaxies, at redshifts 1.132, 1.575, and 2.474 are presented here, with inferred star-formation rates of hundreds of solar masses per year. A series of spectacular coeval AGN/starburst events may have formed these ultra-massive galaxies and their massive central black holes during their relatively short lifetimes.

Subject headings: Galaxies: formation — Galaxies: starburst — Galaxies: high-redshift — Infrared: galaxies

[1]Herschel is an ESA space observatory with science instruments provided by European-led Principal Investigator consortia and with important participation from NASA

1. Introduction

The most massive galaxies known have stellar masses $\sim 5 \times 10^{11}$ $M_\odot$, and the fact that they already exist at early epochs (Fontana et al. 2006) implies that they must have formed rapidly (Daddi et al. 2005), during just a few Giga-years. They are expected to host supermassive black holes (Häring & Rix 2004) which have periods of active accretion (De Breuck et al. 2010). A symbiotic occurrence of modest star-formation and accretion activity has been inferred in the high mass host galaxies of intermediate redshift X-ray selected AGN (Lutz et al. 2010). Additional interest for details of the symbiosis in radio-loud AGN is moreover generated by the proposed negative AGN feedback (e.g., Bower et al. 2006). Here we quantitatively address star-formation and black hole build-up in the most massive galaxies hosting radio-loud AGN, during their time of formation.

Powerful high-redshift radio galaxies are ideal tracers of the extreme form of starburst-AGN symbiosis for several reasons. Firstly, their central black holes are being fed at a high rate, hence are rapidly growing. Secondly, their large extended radio sources allow an unambiguous quantification of the accretion power, from the huge radio luminosities; moreover, their radio morphological properties permit an estimate of the duration of the AGN and possibly coeval star-formation episodes. Thirdly, the presence of large reservoirs of molecular gas, the necessary fuel for star-formation, has been inferred (Solomon & Vanden Bout 2005) from (sub)-millimetre spectroscopy in some radio galaxies (but not in all). Quantification of the ongoing star-formation is provided through far-infrared (FIR) observations, since dust absorbs the radiation of the young stars and re-emits it at FIR wavelengths. From rest-frame submillimetre photometry (Benford et al. 1998; Reuland et al. 2004) and mid-infrared spectral energy distributions, SEDs (Seymour et al. 2008) it was suspected that some powerful high redshift radio galaxies might be experiencing phases of copious (dust obscured) star-formation. The implications from the SED measurements, however, were uncertain: the amount of cool dust reradiating the emission of the newly formed stars was not well constrained, as the rest-frame far-infrared regions and the Rayleigh-Jeans tails lack data.

The Herschel Space Observatory (Pilbratt et al. 2010) provides full measurement of IR-submm SEDs at unprecedented sensitivity. This Letter presents breakthrough results on a sample of seventy radio-loud, high-redshift AGN, namely quasars and radio galaxies from the 3C and 4C catalogues. With $P_{1.4\,\mathrm{GHz}} \sim 10^{27.5}$ W Hz^{-1}, these AGN contain the most powerful accreting black holes. Inspection of our sample measurements shows FIR detection fractions of roughly two in three objects, at both 160μm and 250μm (from the Herschel PACS and SPIRE instruments, respectively). Stressing that the non-detected objects are probably just below the sensitivity limit, we focus here on three archetypal objects, reporting on their spectacular on-going star-formation.

3C 368 (Best et al. 1997, 1998a,b; Chambers & Charlot 1990; Djorgovski et al. 1987), 3C 68.2 (Best et al. 1997, 1998a; Chambers & Charlot 1990; Djorgovski et al. 1988) and 3C 257 (Van Breugel et al. 1998), at redshifts $z = 1.132$, 1.575, and 2.474 respectively, are archetypal protogalaxies with well-documented properties. 3C 257 is the highest redshift object in the complete 3CR sample (Spinrad et al. 1985). The first studies of 3C 68.2 and 3C 368 in the mid and late 1980s, and their

identification as protogalaxies marked the birth of the K–z-diagram (Lilly & Longair 1984) and the beginning of extensive observations of their massive hosts in a cosmological context (Spinrad 1986). The presence of a luminous QSO – a Type-1 AGN, obscured from direct view behind a toroidal circumnuclear dust configuration – was proven in the case of 3C 257 from X-ray data (Derry et al. 2003); similarly the two other objects reveal obscured QSOs, in our as yet unpublished Chandra data.

2. Observations and results

Photometric observations of 3C 368, 3C 68.2 and 3C 257 were carried out as part of a Herschel Guaranteed Time program – see Table 1. The PACS scan-map mode was employed with cross scans in the blue (70μm) and the red (160μm) bands, yielding angular resolution of respectively 5″ and 11″. Data reduction was performed within HIPE (Ott 2010) following standard procedures for deep field observations, including source masking and high-pass filtering. Both scan directions were processed individually and then mosaiced to yield the final map. Aperture photometry (including appropriate aperture corrections) of the sources at the known radio core positions was carried out to measure source flux densities. Photometric uncertainties were determined by measuring the flux in several apertures on empty parts of the background. The SPIRE small map mode was employed in the 250 μm (18″ resolution), 350 μm (25″) and 500 μm (36″) bands. Data processing followed standard procedures for small map data within HIPE. The photometry was performed utilizing a SPIRE source extractor also implemented in HIPE (Savage & Oliver 2007). The uncertainties of the SPIRE photometry are dominated by confusion noise. Combining the Herschel data with our existing (Haas et al. 2008) Spitzer mid-infrared photometry, we were able to trace our science targets as well as other objects in the fields over two decades in wavelength. With this approach we ensure proper identifications while avoiding source confusion. Supplementing our Herschel and Spitzer data with published photometry we obtain the complete optical-IR-submm SEDs. To extract physical parameters, we fitted the data with three components representing typical constituents of a radio galaxy SED. In practice, we started with the AGN-powered warm dust emission by cycling through a library of torus models covering a wide range in the relevant parameter space (Hönig & Kishimoto 2010). For each torus model (using edge-on inclinations of 60°, 75°, or 90°) we added a black body in the optical-NIR for emission from the host galaxy stars[2] as well as a modified black body of variable temperature (grey-body model with β fixed at 1.6) in the FIR/submm to account for possible excess emission due to star-formation. Figure 1 shows for each source the combination of one of the torus models, scaling for all components, and FIR dust temperature which overall minimizes the chi-square, i.e., the best fitting model. Errors on the derived physical parameters were determined from the distribution of these parameter values for the range

[2]3C 257 required the addition of an extra black body of ∼1300 K. Such a component, which is generally identified with hot dust close to the sublimation temperature, is often observed in Type-1 AGN but has not been seen in Type-2s so far. Inclusion or exclusion of this hot dust component does not affect the forthcoming conclusions.

of model combinations consistent with the data. Since radio galaxy jets have large inclinations, radio core emission is relativistically de-boosted rather than boosted as in quasars. Core radio data (Best et al. 1997, 1998b; Van Breugel et al. 1998) indeed show that any non-thermal contribution to the submm emission is negligible. While the SPIRE beam also encloses the radio source hot spots, their contribution is negligible since even the total integrated radio SED underpredicts the FIR/submm by a large margin. As Figure 1 shows, substantial cool dust emission is called for by the SED grey bodies, with temperatures of 53 K, 36 K and 37 K, for 3C 368, 3C 68.2 and 3C 257 respectively. Using standard cosmology ($H_0 = 70$ km s^{-1} Mpc^{-1}, $\Omega_\Lambda = 0.73$, $\Omega_m = 0.27$) we compute source intrinsic properties, which are listed in Table 2. The listed L_{AGN}-values originate from the torus modeling: they represent the (accretion) luminosities required to power the fitted torus emission. The L_{SF}-values were determined by integrating the fitted FIR grey bodies between 8μm and 1000μm.

3. Discussion

In analogy with other studies (Benford et al. 1998; Hatziminaoglou et al. 2010) we attribute the torus heating, i.e., the warm dust component, to the obscured AGN: their luminosities are $\sim 10^{46}$ erg sec^{-1}, confirming the luminous active accretion in these radio-loud Type-2 AGN, which is consistent with the unification scenario (Barthel 1989; Derry et al. 2003; Haas et al. 2004; Ogle et al. 2006). Attributing the cool dust emission to star-formation, we determine luminosities which are comparable to the AGN luminosities (Table 2), all in excess of 10^{12} L$_\odot$. Using standard conversions (Kennicutt 1998), the star-formation rate (SFR) values are 610, 390 and 770 M$_\odot$ yr^{-1}, for 3C 368, 3C 68.2 and 3C 257, respectively. Hence, all three high-z radio galaxies are prodigious star-formers[3]. Four points are noteworthy: (1) when comparing the SFRs with values inferred from uv/optical data (Chambers & Charlot 1990) we conclude that most of the star-formation in these three objects is strongly obscured in that band, (2) as judged from their radio sizes (this point will also return later), these are mature objects rather than young AGN in a transition phase from dust obscured infrared galaxies to AGN, (3) 3C 68.2 and 3C 257 have cool dust temperatures in the range of those measured for distant sub-millimetre galaxies (Magnelli et al. 2012), and (4) as judged from the detection statistics ($\sim$ 70%), many (if not all) of our sample objects must have optically obscured star-formation of comparable strength, i.e., SFRs of hundreds of M$_\odot$ yr^{-1}. The high star-formation luminosities for these high-z radio galaxies are consistent with results from deep field Herschel surveys targeting a mix of radio-quiet AGN types over a large redshift range out to $z \sim 3$ (Hatziminaoglou et al. 2010; Elbaz et al. 2010; Mullaney et al. 2012a) and with results from $z > 4$ QSO studies (Leipski et al. 2010), but our detection fraction is higher.

[3]For comparison, we performed the same decomposition for the host of the powerful low-redshift radio galaxy Cygnus A (3C 405), using published (Haas et al. 2004) SED data, finding considerably lower values: $L_{AGN} = 8.2 \times 10^{44}$ erg sec^{-1} and $L_{SF} = 1.5 \times 10^{11}$ L$_\odot$ (SFR 26 M$_\odot$ yr^{-1}).

Our observations indicate that many distant powerful radio galaxies display star-formation at a level comparable to ultra-luminous infrared galaxies (ULIRGs) which is coeval to their black hole activity. That conclusion together with the above mentioned results of Herschel studies dealing with powerful radio-quiet AGN are in marked contrast with the conclusion (Page et al. 2012) for X-ray selected $1 < z < 3$ (radio-quiet) AGN in the CDF-N, namely that ultra-luminous starburst activity is not seen in the most powerful AGN. While detailed comparison of these conflicting results is beyond the scope of this Letter we point out two possible explanations. Firstly, the hosts of the CDF-N AGN are of lower stellar mass than the radio source hosts. We stress that distant 3C and 4C objects (of which only of order 10^2 are known) represent the highest peaks in the galaxy mass distribution. In fact, our observations are in broad agreement with the extrapolated cosmologically evolving specific SFR, sSFR, in the hosts of luminous AGN (and star-forming galaxies) recently established by Mullaney et al. (2012a). A – puzzling – inverse correlation between AGN X-ray strength and host galaxy mass would be required to explain the Page et al. (2012) results within the just mentioned sSFR behaviour in combination with our findings for radio-loud AGN. Secondly, radio-selected AGN – selected using radio lobe luminosity which is an isotropic property – represent a cleaner, more complete AGN subsample than do X-ray-selected AGN: the latter may lack the most obscured sources. The X-ray luminosities reported by Page et al. (2012) are uncorrected for obscuration, who estimate the effect is small. X-ray observations for the 3C sources reported here indicate observed luminosities, assuming a standard power-law spectrum with $\Gamma = 1.9$, of about 3×10^{43} erg s^{-1}, 4×10^{43} erg s^{-1} (Wilkes et al., 2012, in prep.) and 1.5×10^{44} erg s^{-1} (Derry et al. 2003) for 3C 68.2, 3C 368 and 3C 257 respectively, comparable with sources in the Page et al. (2012) sample. It is well known that low signal-to-noise (S/N) X-ray data provide poor estimates of obscuration and so result in luminosities uncertain by 1–2 dex (Cappi et al. 2006; Wilkes et al. 2005). Indeed, for all three 3C sources reported here (radio galaxies), the X-ray data indicate significant obscuration with estimated $N_H \sim 10^{23-24}$, yielding estimated intrinsic, hard-band X-ray luminosities of $\sim 10^{45}$ erg s^{-1} for 3C 68.2 and 3C 368 (Wilkes et al., 2012, in prep.) and 9×10^{44} erg s^{-1} for 3C 257 (2–10 keV, Derry et al. (2003)). The low S/N of the X-ray data combined with the likely presence of additional, unobscured, radio-jet-linked emission (responsible for the typically 3× brighter X-ray luminosities in radio-loud quasars, Zamorani et al. (1981)) make it likely that the N_H and intrinsic X-ray luminosity for these three 3C sources remain underestimated. Although X-ray emission in radio-quiet AGN is less complex and may be somewhat lower luminosity, the stronger bias against highly-obscured sources and the difficulty in detecting absorption in the fainter X-ray sources, which are those most likely to be obscured (Kim et al. 2007), is very likely to result in significantly underestimated X-ray luminosities in the Page et al. X-ray-selected sample. The fact that a higher incidence of X-ray absorption in those sources with 250μm detections is also reported strengthens this possibility and so questions their main conclusion: that 250 μm emission is undetected, indicating that SF is quenched, in the highest luminosity, $L_X \gtrsim 10^{44}$ erg s^{-1}, active galaxies in their sample. Careful examination of the true nature of the high-z X-ray AGN is required to back-up the proposed negative feedback; such feedback is definitely not observed in the radio-loud(est) AGN. While the duration of the vigorous star-formation phase could be longer than the

radio-loud activity episode, with the star-formation starting earlier than and possibly eventually being quenched by the AGN (analysis of our full sample of young, mature and old radio sources will address that issue), based on our observations there is a substantial symbiotic period.

In contrast to other AGN, radio galaxies – with their extended radio structure at high inclination – offer the unique possibility of estimating the age of the activity episode from the linear size of the structure, adopting a typical (Best et al. 1995) source expansion speed of ten to twenty per cent of the speed of light. The average duration of such an episode follows from the maximum size of radio galaxies at the relevant cosmic epoch. Then 3C 68.2, measuring ∼190kpc, has a large dimension implying its AGN phase has an age of several million years, while the sizes of 3C 368 and 3C 257 indicate that they are somewhat younger. Focussing on 3C 68.2, and adopting an AGN age of 5 Myr, a symbiotic star-formation phase at the inferred SFR of ∼500 $M_\odot$ yr^{-1}, assuming it to be constant, would yield $\sim 2.5 \times 10^9$ $M_\odot$. The actual figure could be larger if the star-formation commenced before the AGN phase. The host mass of 3C 68.2, 5×10^{11} $M_\odot$ (Best et al. 1998a), can be formed through ∼200 such gas accretion phases, for which there is sufficient time given the age of the universe at that redshift of 4 Gyr. The ∼200 associated AGN phases will last a total time of $\sim 10^9$ yr during which a massive central black hole of $\sim 1 \times 10^9$ $M_\odot$ must accrete (Häring & Rix 2004). The implied average black hole fuel consumption of 1 $M_\odot$ yr^{-1} yields an energy output $\sim \eta.\mathrm{dm/dt}.c^2$ which for a typical accretion efficiency $\eta = 0.1$ equals 5×10^{45} erg sec^{-1} – about a factor seven below the observed AGN luminosity of 3C 68.2. An essential element in this discussion is the assumption that the growth of the central black hole during AGN episodes is in phase with the build-up of its host galaxy. We cannot exclude the possibility of a more energetic star-forming phase (for instance at SFR $\sim 10^4$ $M_\odot$ yr^{-1}), but such SFRs remain to be observed in high-redshift radio galaxies. However, if the star-forming phase lasts about a factor ten longer than the symbiotic phase, then ∼20 such events are needed to build-up the massive galaxy. In that case the mass consumption required to build its black hole during the ∼20 AGN episodes would be in agreement with the measured AGN luminosity. Other forms of symbiotic occurrences can also be envisaged, including pure AGN phases not linked to coeval starbursts and the direct capture of stars through galaxy-galaxy merging. Whereas low redshift ULIRGs are believed to originate from major mergers, high redshift ULIRGs in the form of submm galaxies might have formed through cold gas accretion (Davé et al. 2010); the same has been postulated for high redshift AGN (Bournaud et al. 2011). Even at their extreme stellar masses, our 3C hosts obey the sSFR(z) behaviour for non-AGN and X-ray AGN (Mullaney et al. 2012a). However, their X-ray luminosities are higher, by orders of magnitudes; moreover they are radio-loud. They may well mark the rare, most extreme examples of the universal accretion to star-formation rate ratio postulated by Mullaney et al. (2012b). Following these authors, we contend that the full symbiosis whereby a cold gas inflow driven, vigorous star-formation episode leads into (and may be quenched by) an energetic AGN phase, offers an attractive scenario for the reason of a common fuel supply, building up both black hole and stellar mass.

4. Conclusions

Following implications from submm emission, mid-IR spectra and Ly-α emission, we now know unambiguously that a substantial fraction of the hosts of high-redshift radio galaxies are dust and gas rich, undergoing one of likely many phases of copious star-formation. Energetically speaking they are comparable to ultra-luminous infrared galaxies. Our study shows accretion and star-formation activity simultaneously at work in the most massive early-epoch galaxies, building these galaxies and their central black holes, forcefully and effectfully. It will be important to extend the investigations to radio-loud AGN hosted by less massive galaxies. Radio-loud activity phases must play an important role in galaxy formation.

The Herschel spacecraft was designed, built, tested, and launched under a contract to ESA, managed by the Herschel/Planck Project team, by an industrial consortium under the overall responsibility of the prime contractor Thales Alenia Space (Cannes), and including Astrium (Friedrichshafen) responsible for the payload module and for system testing at spacecraft level, Thales Alenia Space (Turin) responsible for the service module, and Astrium (Toulouse) responsible for the telescope, with in excess of a hundred subcontractors. HCSS/HSpot/HIPE is a joint development by the Herschel Science Ground Segment Consortium, consisting of ESA, the NASA Herschel Science Center, and the HIFI, PACS and SPIRE consortia. We acknowledge the support and interest of the full Guaranteed Time Proposal team, of Dutch liaison astronomer Max Avruch, of colleague Karina Caputi, and the comments of an expert referee.

REFERENCES

Barthel, P. D. 1989, ApJ, 336, 606

Benford, D. J., et al. 1999, ApJ, 518, L65

Best, P. N., et al. 1995, MNRAS, 275, 1171

Best, P. N., et al. 1997, MNRAS, 292, 758

Best, P. N., et al. 1998a, MNRAS, 295, 549

Best, P. N., et al. 1998b, MNRAS, 299, 357

Bournaud, F., et al. 2011, ApJ, 741, L33

Bower, R. G., et al. 2006, MNRAS, 370, 645

Cappi, M., et al. 2006, A&A, 446, 459

Chambers, K. C., & Charlot, S. 1990, ApJ, 348, L1

Daddi, E., et al. 2005, ApJ, 631, L13

Davé, R., et al. 2010, MNRAS, 404, 1355

Derry, P. M., et al. 2003, MNRAS, 342, L53

Djorgovski, S., et al. 1987, AJ, 93, 1307

Djorgovski, S., et al. 1988, AJ, 96, 836

De Breuck, C., et al. 2010, ApJ, 725, 36

Elbaz, D., et al. 2010, A&A, 518, L29

Fontana, A., et al. 2004, A&A, 459, 745

Haas, M., et al. 2004, A&A, 424, 531

Haas, M., et al. 2008, ApJ, 688, 122

Häring, N., & Rix, H.-W. 2004, ApJ, 604, L89

Hatziminaogou, E., et al. 2010, A&A, 518, L33

Hönig, S. F., & Kishimoto, M. 2010, A&A, 523, A27

Kennicutt Jr, R. C. 1998, ARA&A, 36, 189

Kim, M., et al. 2007, ApJ, 659, 29

Leipski, C., et al. 2010, A&A, 518, L34

Lilly, S. J., & Longair, M. S. 1984, MNRAS, 211, 833

Lutz, D., et al. 2010, ApJ, 712, 1287

Magnelli, B., et al. 2012, A&A, 539, A155

Mullaney, J. R., et al. 2012a, MNRAS, 419, 95

Mullaney, J. R., et al. 2012b, ApJ, 753, L30

Ogle, P., et al. 2006, ApJ, 647, 161

Ott, S. 2010, Astronomical Data Analysis Software and Systems XIX, 434, 139

Page, M. J., et al. 2012, Nature, 485, 213

Pilbratt, G. L., et al. 2010, A&A, 518, L1

Reuland, M., et al. 2004, MNRAS, 353, 377

Savage, R. S., & Oliver, S. 2007, ApJ, 661, 1339

Seymour, N., et al. 2008, ApJ, 681, L1

Solomon, P. M. and Vanden Bout, P. A. 2005, ARA&A, 43, 677

Spinrad, H., et al. 1985, PASP, 97, 932

Spinrad, H. 1986, PASP, 98, 269

Van Breugel, W. J. M., et al. 1998, ApJ, 502, 614

Wilkes, B. J., et al. 2005, ApJ, 634, 183

Zamorani, G., et al. 1981, ApJ, 245, 357

Table 1. Observations and measured flux densities. Herschel observations using the PACS and SPIRE instruments yielded photometric data in five bands. The 1-sigma errors combine the measurement noise and the background noise.

Object	RA(J2000)	DEC(J2000)	Obs.date	Obs.band	Integr.time	Flux density (mJy)
3C 368	$18^{h}05^{m}06\overset{s}{.}36$	$+11°01'32\overset{''}{.}5$	2011 March 22	70μm	160sec	30.0±2.0
			2011 March 22	160μm	160sec	56.0±3.0
			2011 March 28	250μm	111sec	31.1±7.0
			2011 March 28	350μm	111sec	20.1±6.6
			2011 March 28	500μm	111sec	<21.0
3C 68.2	$02^{h}34^{m}23\overset{s}{.}86$	$+31°34'17\overset{''}{.}5$	2011 July 10	70μm	160sec	27.0±6.0
			2011 July 10	160μm	160sec	40.0±7.0
			2011 July 31	250μm	111sec	28.7±7.1
			2011 July 31	350μm	111sec	29.6±7.4
			2011 July 31	500μm	111sec	19.7±7.0
3C 257	$11^{h}23^{m}09\overset{s}{.}17$	$+05°30'19\overset{''}{.}5$	2011 June 1	70μm	640sec	11.6±1.0
			2011 June 1	160μm	640sec	16.0±1.7
			2010 Nov 23	250μm	296sec	22.8±4.9
			2010 Nov 23	350μm	296sec	20.1±5.7
			2010 Nov 23	500μm	296sec	20.4±6.8

Table 2. AGN and star-formation luminosities. The inferred AGN and star-formation luminosities for the three high-redshift radio galaxies are listed, as well as their (projected) radio source sizes and host galaxy masses, taken from the literature (with references). The 1-sigma errors were determined from the distribution of the ten best model combination sets.

Object	Redshift	T_{cool} (K)	L_{AGN} (erg sec^{-1})	L_{SF} (erg sec^{-1})	L_{SF} (10^{12} $L_{\odot}$)	SFR ($M_{\odot}$ yr^{-1})	Radio size (kpc)	M_{host} ($M_{\odot}$)	M_{host}/radio refs.
3C 368	1.132	53±1	$(7.3\pm3.5)\times10^{45}$	$(1.4\pm0.04)\times10^{46}$	3.5±0.1	610	80	$10^{11.6}$	Best et al. (1998a,b)
3C 68.2	1.575	36±3	$(3.3\pm1.0)\times10^{46}$	$(8.6\pm0.8)\times10^{45}$	2.2±0.2	390	190	$10^{11.7}$	Best et al. (1997, 1998a)
3C 257	2.474	37±3	$(4.1\pm2.0)\times10^{46}$	$(1.7\pm0.1)\times10^{46}$	4.4±0.3	770	95	$< 10^{11.7}$	De Breuck et al. (2010); Van Breugel et al. (1998)

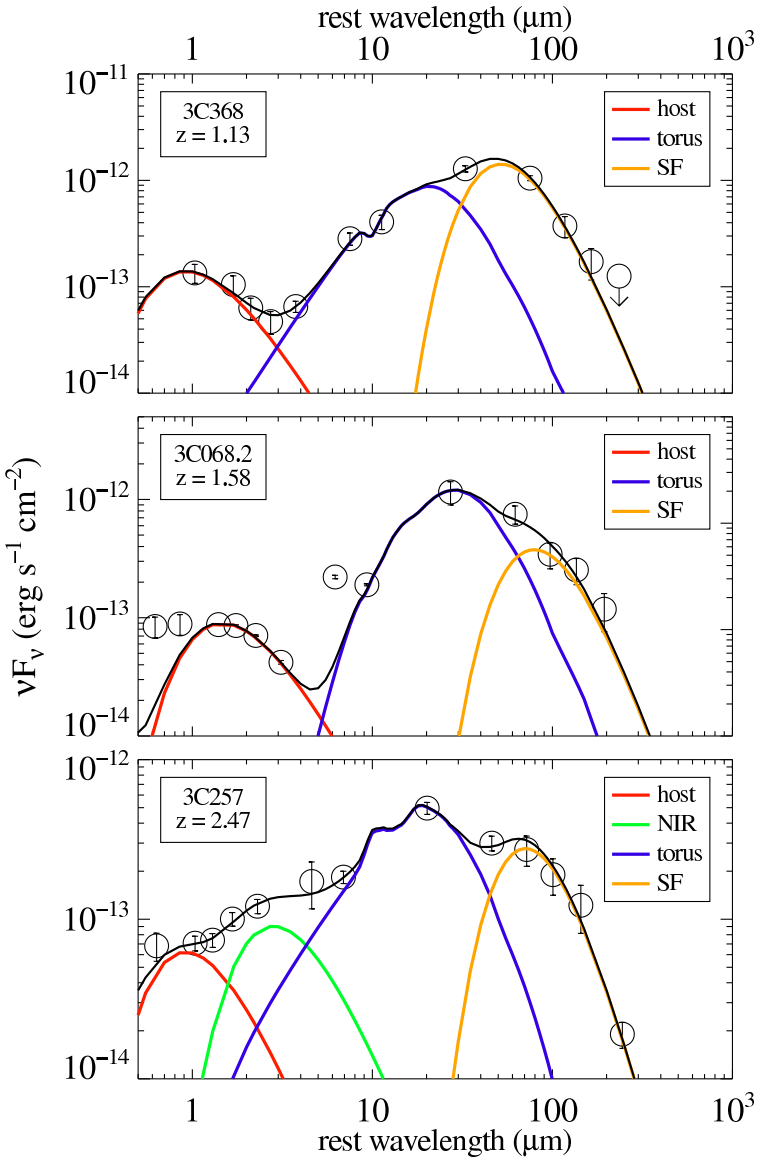

Fig. 1.— Infrared-submm spectral energy distributions. The infrared-submm SEDs of 3C 368, 3C 68.2, and 3C 257 are shown, with the best-fitting, multi-component model superposed: stellar radiation (red), torus radiation (blue), and cool dust radiation (yellow). 3C 257 requires an extra hot dust component (green) – see the main text. The mismatch at 16μm for 3C 68.2 is possibly due to luminous PAH-emission. The error bars reflect $\pm 1\sigma$ errors.